Energy Conversion and Management: X 28 (2025) 101251

Contents lists available at ScienceDirect

Energy Conversion and Management: X

journal homepage: www.sciencedirect.com/journal/energy-conversion-and-management-x

Evaluating cost and emission reduction potentials with stochastic PPA portfolio optimization for green hydrogen production in a decarbonized glassworks

Jonas Brucksch [a,b,c,d,*], Jonas van Ouwerkerk [a,b,c,d], Dirk Uwe Sauer [a,b,c,d,e]

[a] *Chair for Electrochemical Energy Conversion and Storage Systems, Institute for Power Electronics and Electrical Drives (ISEA), RWTH Aachen University, Aachen, Germany*
[b] *Institute for Power Generation and Storage Systems (PGS), E.ON ERC, RWTH Aachen University, Aachen, Germany*
[c] *Center for Ageing, Reliability and Lifetime Prediction for Electrochemical and Power Electronic Systems (CARL), RWTH Aachen University, Aachen, Germany*
[d] *Jülich Aachen Research Alliance, JARA-Energy, Aachen, Germany*
[e] *Forschungszentrum Jülich GmbH, Institute of Energy and Climate Research Helmholtz-Institute Münster: Ionics in Energy Storage (IMD-4), Jülich, Germany*

ARTICLE INFO

Keywords:
Green hydrogen
PPA
MILP
Stochastic optimization
Glassworks
Battery energy storage system

ABSTRACT

The decarbonization of heavy industries demands large volumes of green hydrogen. To produce green hydrogen via electrolysis, the EU's Renewable Energy Directive II imposes rules to ensure the use of renewable electricity. Hydrogen producers can use portfolios of power purchase agreements (PPAs) to buy renewable electricity. These portfolios must meet hydrogen demand cost-effectively, and battery storage can help by shifting excess renewable generation. However, high uncertainty around future electricity prices and demand complicates optimal portfolio design. Current literature lacks comprehensive models that evaluate such portfolio optimization under uncertainty for real-world case studies including battery storage. This work addresses the gap by introducing a stochastic mixed-integer linear programming model tailored to industrial applications. We demonstrate the model using a real-world glass manufacturing site in Germany. Our findings show that portfolio optimization alone can reduce the levelized cost of hydrogen (LCOH) by 6.24% under EU rules. Adding a battery further cuts costs, achieving an LCOH of 11.8 $€_{2024}$ kg^{-1}. Exploring different temporal matching schemes reveals that weekly matching reduces LCOH by 2 $€_{2024} kg^{-1}$ while maintaining a high share of renewable energy. The model offers a flexible tool for optimizing PPA portfolios in various industrial settings.

1. Introduction

The industrial sector accounts for roughly 18% of Germany's greenhouse gas (GHG) emissions in 2022 [1], making its decarbonization a central step toward climate neutrality. Within this sector, the glass industry alone emitted 3.9 Mt of CO_2 in 2022 [2]. Since around 80% of the total energy demand in glass manufacturing is required for material heating, replacing natural gas in conventional furnaces with CO_2-neutral alternatives represents a particularly promising pathway. Among these, green hydrogen has received considerable attention from both industry and academia [3,4], and several demonstration projects are currently under way [5–7].

However, the climate benefits of hydrogen depend strongly on how it is produced. Different electricity generation processes result in widely varying costs and emissions [8]. To address this, the European Union's Renewable Energy Directive II (RED2) defines strict criteria for renewable hydrogen production, including additionality, simultaneity, and geographical proximity between renewable electricity generation and consumption [9]. In particular, the simultaneity requirement will demand hourly matching between renewable generation and electrolyzer consumption from 2030 onwards, raising concerns about economic feasibility [10]. During the transition period until 2030, a monthly matching rule applies.

Power purchase agreements (PPAs) offer one mechanism to satisfy these requirements while securing long-term renewable supply. PPAs are bilateral contracts between electricity producers and consumers that define quantities, prices, and risk allocation. Common structures include Pay-as-Produced (PaP) PPAs, where the off-taker purchases a fixed share of renewable generation at each time step, and baseload PPAs, where a constant volume is supplied each hour. Baseload PPAs

* Corresponding author at: Chair for Electrochemical Energy Conversion and Storage Systems, Institute for Power Electronics and Electrical Drives (ISEA), RWTH Aachen University, Aachen, Germany.
E-mail address: jonas.bruckschisea.rwth-aachen.de (J. Brucksch).

https://doi.org/10.1016/j.ecmx.2025.101251
Received 3 July 2025; Received in revised form 3 September 2025; Accepted 4 September 2025
Available online 15 September 2025

provide higher supply security but are typically more expensive than PaP PPAs [11]. Initially developed in the U.S. and Northern Europe to support renewable project financing, PPAs are now widespread in Germany, Spain, and the Nordic countries [12].

While PPAs facilitate renewable procurement, they also involve challenges. Contracts typically span 5–10 years [13], requiring careful alignment with future electricity needs and price developments. Misjudgments can impose significant financial burdens on energy-intensive industries such as glass manufacturing. Moreover, uncertainties in future market prices, renewable generation profiles, and industrial consumption complicate PPA portfolio selection. Addressing these uncertainties requires robust optimization approaches.

Scenario-based two-stage stochastic optimization provides such a framework. In the first stage, strategic decisions such as PPA selection are made before uncertainties unfold; in the second stage, operational decisions such as dispatch adjustments are optimized for realized scenarios. This allows for robust solutions across a wide range of possible futures, outperforming deterministic one-stage models that rely on a single forecast [14,15]. For industrial off-takers, this method can significantly enhance long-term economic stability.

Battery energy storage systems (BESS) further increase the flexibility of PPA-based procurement. By shifting surplus renewable electricity from periods of high availability to times of scarcity, batteries allow industries to rely more on cost-effective PaP PPAs instead of more expensive baseload contracts. Industrial stationary battery capacity has expanded rapidly in recent years—growing by 372% between 2022 and 2024 in Germany alone, from 200 MWh to 743 MWh [16]. In industrial applications, batteries are already used for peak shaving and optimizing self-consumption; extending their role to PPA integration can unlock additional value.

Existing literature provides valuable insights into renewable procurement strategies, but also reveals key gaps. Brandt et al. analyze the impact of RED2 on hydrogen production costs under different matching rules but do not consider storage or spatially diverse generation [10]. Gabrielli et al. compare PPA portfolios across countries [17], while Riepin et al. examine 24/7 clean energy procurement [18], yet both neglect hydrogen-specific industrial contexts. Casas Ferrús et al. demonstrate portfolio effects for hydrogen producers in Germany [19], and Gabrielli et al. highlight the benefits of co-locating storage with renewables [20], but neither focus on industrial off-takers or RED2 simultaneity. Other studies explore hybrid renewable–hydrogen systems using advanced optimization methods [21–23], but lack explicit scenario-based analysis of uncertainty or application-specific insights for German industry.

To date, no study has analyzed how industrial hydrogen producers in Germany can jointly optimize PPA portfolios, battery storage, and electrolyzer capacity under RED2 simultaneity constraints.

This work addresses that gap by developing a stochastic two-stage optimization model that integrates PPA contracting, energy storage, and electrolyzer sizing. Our model explicitly incorporates uncertainties in renewable generation and hydrogen demand, and evaluates up to 50 PPA options characterized by spatio-temporal weather and technology-specific cost data. By modeling RED2's temporal matching rules, we analyze their implications for hydrogen producers. We apply the framework to a realistic case study of a German glassworks with time-dependent hydrogen demand, demonstrating how PPAs and batteries can be leveraged synergistically to achieve cost-effective, RED2-compliant hydrogen production.

The remainder of this paper is structured as follows. Section 2 introduces the stochastic optimization model. Section 3 describes the case study based on data from a German glassworks. Section 4 analyzes the effects of portfolio size, storage integration, and RED2 simultaneity rules on hydrogen production costs. Section 5 concludes the paper.

2. Methodology

This section introduces the mathematical formulation of the optimization problem. We build a two-level optimization problem to consider uncertainties like weather conditions, price variations, and exact demand values. The first stage determines component capacities, while the second stage optimizes all scenario- and time-dependent variables. Furthermore, we use a mixed-integer linear program formulation for the optimization problem as these programs have been proven to be a viable option for such large-scale problems under uncertainty [24]. We start with a detailed description of the modeled energy system. It continues with the formulation of the constraint to realize different temporal matching requirements for electricity procurement. The next section describes the objective function in detail. The final section introduces multiple key performance indicators for the analysis of the optimization results.

2.1. Industrial energy system

The energy system of a hydrogen producer can be split into a front-of-the-meter (FTM) and a behind-the-meter (BTM) part. FTM activities are consolidated within the company's balancing circle (BLC), incorporating all virtual electricity trading transactions. The residual quantity of traded electricity passes through the company's BTM grid connection point. For all BTM electricity, we distinguish between electricity demand for the green hydrogen production and other electricity demand that the company has (Eq. (1)). With this, it is possible to realize special legal requirements like temporal matching or exemption from levies that only apply to electricity for green hydrogen production.

Eqs. (2) to (9) describe all FTM activities for every timestep t of the optimized time horizon T in scenario s. The total PPA electricity $P_{t,s}^{PPA}$ at every timestep t in scenario s splits into baseload $P^{PPA,Base}$, PV $P^{PPA,PV}$ or wind power PPAs $P^{PPA,Wind}$. The power flow variable P^{import} between the BTM-busbar and the BLC represents the physically imported electricity considering the efficiency of the grid connecting transformer η_{Traf}. The hydrogen producer can procure electricity at a public market $P^{DA,buy}$ or via PPA contracts from different RES locations from PV generators L_{pv} or wind generators L_w. With a PaP PPA contract, the buyer must take all electricity generated in the RES. Thus, the amount of bought electricity from each location depends on the contract size $S_l^{PPA,res}$ between the off-taker and the generator and the power factors $PF_l^{PPA,res}$ of location l. An efficiency η represents additional losses through power conversion and transportation from the generator to the off-taker location. For each possible PaP contract, there exists a binary variable b that defines if a contract has been signed with a generator or not. As the electricity bought from the PPA contracts does not always match the demand, excess electricity may be sold at the public market $P^{DA,sell}$, curtailed $P^{curtail}$ or used for matching other electricity demands of the off-taker not connected to the hydrogen production D^{other}. Finally, constraints (5) to (8) ensure that only a certain amount of PPAs can be chosen from all locations L. Here, the parameter M is a large value enabling the bigM method [25]. Constraint (9) sets the power purchased from the baseload PPA contract $P^{PPA,Base}$ exactly at the contracted power of that contract $S^{PPA,Base}$ for every timestep.

$$P^{import} = P_{t,s}^{ProdH_2} + D_{t,s}^{other} \tag{1}$$

$$P_{t,s}^{PPA} = \sum_{l\in L_{pv}} P_{l,t,s}^{PPA,PV} + \sum_{l\in L_w} P_{l,t,s}^{PPA,Wind} + P_{t,s}^{PPA,Base} \tag{2}$$

$$P_{t,s}^{import} = (P_{t,s}^{DA,buy} - P_{t,s}^{DA,sell} + P_{t,s}^{PPA} - P_{t,s}^{curtail}) \cdot \eta_{Traf} \tag{3}$$

$$P_{l,t,s}^{PPA,PV} = \eta_{PPA} \cdot PF_{l,t,s}^{PV} \cdot S_l^{PPA,PV} \forall l \in L_{pv} \tag{4}$$

$$S_l^{PPA,PV} \leq b_l^{PV} \cdot M \quad \forall l \in L_{pv} \tag{5}$$

$$P_{l,t,s}^{PPA,Wind} = \eta_{PPA} \cdot PF_{l,t,s}^{Wind} \cdot S_l^{PPA,Wind} \quad \forall l \in L_w \tag{6}$$

$$S_l^{PPA,Wind} \leq b_l^{Wind} \cdot M \quad \forall l \in L_w \tag{7}$$

$$n_{max}^{PPA} \geq \sum_{l \in L} \left(b_l^{PV} + b_l^{Wind} \right) \tag{8}$$

$$P_{t,s}^{PPA,Base} = S^{PPA,Base} \tag{9}$$

When optimizing electricity procurement with perfect foresight of electricity prices, the solver tries to use price incentives as much as possible. In practice, however, a company would never do so as they cannot predict prices perfectly. To restrict the solver from buying surplus amounts of PPAs to sell them with profit on the day-ahead market with unrealistically high revenue, Eq. (10) limits the sold energy to a certain share $f_{sell,max}$ of the electricity demand [18].

$$\sum_{tinT} (P_{t,s}^{ELY} + D_{t,s}^{other}) \cdot f_{sell,max} \leq \sum_{t \in T} P_{t,s}^{DA,sell} \tag{10}$$

Eqs. (11) to (13) specify BTM activities for green hydrogen production. The total power used to produce hydrogen $P^{Prod H_2}$ is divided into charging or discharging the battery ($P^{BAT,cha}$ and $P^{BAT,dch}$) as well as operating an electrolyzer P^{ELY}. The hydrogen production must serve a given time- and scenario-dependent hydrogen demand D^{H_2} considering a fixed electrolysis efficiency of η_{ELY}. The hydrogen demand is given in power values for each optimization time step. A hydrogen pressure storage PS can be used to store hydrogen after production $P^{ELY,PS}$ or releasing it to serve the H_2 demand (Eq. (13)). Constraint (14) limits the electrolyzer's power input to the component's size.

$$P_{t,s}^{ELY} + P_{t,s}^{BAT,cha} = P_{t,s}^{BAT,dch} + P_t^{Prod H_2} \tag{11}$$

$$P_{t,s}^{ELY} \cdot \eta_{ELY} = P_{t,s}^{ELY,PS} + P_{t,s}^{ELY,H_2} \tag{12}$$

$$D_{t,s}^{H_2} = P_{t,s}^{ELY,H_2} + P_{t,s}^{PS,H_2} \tag{13}$$

$$P_{t,s}^{ELY} \leq S^{ELY} \tag{14}$$

Furthermore, Eq. (15) declares a variable describing the peak demand increase for the hydrogen production, assuming that a certain power limit for the grid connection point S^{GCP} is already in place.

$$P_{t,s}^{import} - S^{GCP} \leq P_s^{PeakIncrease} \tag{15}$$

The constraints (16) to (19) are valid for each storage component STR which is the battery storage (BAT) or the pressure storage (PS). First, input and output power flows determine the current energy level $E_{t,s}^{STR}$ considering the energy level from the previous timestep $E_{t-1,s}^{STR}$ charging and discharging activities with corresponding efficiencies η_{cha}^{STR} and η_{dch}^{STR} for charging and discharging, respectively. Furthermore, the E2P ratio limits the power that can be delivered in each timestep through constraints (17) and (18) depending on the optimized size of the component S^{STR}. Finally, constraint (19) limits the energy level of the storage to the fixed storage size S^{STR} and the given energy-to-power ratio $e2p^{STR}$. Both storages have fixed efficiencies η_{cha}^{STR} and η_{dch}^{STR} for charging and discharging, respectively.

$$E_{t,s}^{STR} = E_{t-1,s}^{STR} + P_{t,s}^{STR,cha} \cdot \eta_{cha}^{STR} - \frac{P_{t,s}^{STR,dch}}{\eta_{dch}^{STR}} \tag{16}$$

$$P_{t,s}^{STR,cha} \leq S^{STR}/e2p^{STR} \tag{17}$$

$$P_{t,s}^{STR,dch} \leq S^{STR}/e2p^{STR} \tag{18}$$

$$0 \leq E_{t,s}^{STR} \leq S^{STR} \tag{19}$$

2.2. Temporal matching

Following the RED2 regulations different temporal restrictions exist in the future for green hydrogen production [9]. This work assumes that following the RED2 directive, electricity may only taken from the grid in two cases: (1) In times when the day-ahead price is lower than 20 €$_{2024}$ MWh^{-1}. In these times, the factor $b_{DA,t}$ has the value 1, at all other times 0. (2) The electricity has been produced in RES contracted via a PPA (PV, Wind or baseload).

The bought electricity under the two conditions listed above must comply with a temporal matching condition. The temporal matching defines the duration in which the sum of the green electricity bought by an off-taker has to surpass the electricity needed for green hydrogen production. Until 2030, green electricity production from PPAs must match the demand for hydrogen production only on a monthly scale. However, from then onwards, this temporal matching constraint is to be fulfilled every hour of the year. Eq. (20) incorporates temporal matching regulations where n represents the number of hours in which the green supply has to surpass the demand and T_{match} is the number of matching periods in that regulation scheme. The formulation can be adjusted by changing n and T_{match} to represent different regulation standards. For an hourly matching n would have the value $n = 1$ and T_{match} would be every hour of the year with values from 1 to 8760. In a monthly matching scheme, n would have the value $n = 720$ assuming a matching period of 30 days while T_{match} takes values from 1 to 12.

$$\sum_{t=t_0 \cdot n}^{(t_0+1)\cdot n} P_{t,s}^{Prod H_2} <= \sum_{t=t_0 \cdot n}^{(t_0+1)\cdot n} P_{t,s}^{DA,buy} \cdot b_{DA,t} + P_{t,s}^{PPA}, \forall t_0 \in [1, T_{match}] \tag{20}$$

2.3. Objective

The objective function for the stochastic portfolio optimization minimizes the expected annual costs over all scenarios s. For this, component investment costs are transferred to annual costs using the annuity method. The overall formulation in Eq. (21) adds annual capital costs (CAPEX, for component investments) and operating costs (OPEX). As the operating costs are scenario-dependent, the mean value over all scenarios is minimized where n_s is the total number of scenarios. This approach ensures that every scenario is given equal weight.

$$\begin{aligned} \min \quad & C^{CAPEX} + \mathbb{E}(C_s^{OPEX}) \\ & = \min \left(C^{CAPEX} + \frac{1}{n_s}(C_s^{PPA} + C_s^{DA} + C_s^{PeakIncrease}) \right) \end{aligned} \tag{21}$$

$$C^{CAPEX} = C_{bat} + C_{ELY} + C_{PS} \tag{22}$$

The CAPEX part includes costs for installing the battery system C_{bat}, the electrolyzer C_{ELY}, and the pressure storage C_{PS} (Eq. (22). The OPEX consist of multiple cost factors namely costs for procuring electricity from PPAs C^{PPA} or the Day-Ahead market C^{DA} as well as potential costs from higher peak demands $C^{PeakIncrease}$. In the calculation of PPA costs in (23), specific costs are used for each PPA type (PV, wind, or baseload) with the respective amount of purchased electricity for each hour. For the day-ahead market, Eq. (24) introduces a spread c_{tr} between sell and buy price p^{DA} at this market to consider transaction costs for market participation fees or third-party services [26]. Finally, the increase of peak demands can come with extra costs e.g. for expanding transformation infrastructure which is accounted for by the costs factor $c^{PeakIncrease}$.

$$\begin{aligned} C^{PPA} = & \sum_{l \in Lpv; t \in T; s \in S} p^{PPA,PV} \cdot P_{l,t,s}^{PPA,PV} \\ & + \sum_{l \in L_w; t \in T; s \in S} p^{PPA,Wind} \cdot P_{l,t,s}^{PPA,Wind} \\ & + \sum_{t \in T} p^{PPA,Base} \cdot P_t^{PPA,Base} \end{aligned} \tag{23}$$

$$C^{DA} = \sum_{t \in T; s \in S} p_{t,s}^{DA} \cdot P_{t,s}^{DA,buy} - (p_{t,s}^{DA} - c_{tr}) \cdot P_{t,s}^{DA,sell} \tag{24}$$

$$C^{PeakIncrease} = \sum_{s \in S} P_s^{PeakIncrease} \cdot c^{PeakIncrease} \tag{25}$$

2.4. Performance indicators

This chapter explains various parameters that are used to evaluate the results. The Levelized Cost of Hydrogen (LCOH) and Electricity

(LCOE) are used to assess the costs of the energy system using comparable benchmarks. The CEF and CO_2 emissions are used to analyze the ecological impact of the system.

2.4.1. Levelized costs

Levelised costs are a metric used to measure costs per unit produced. As hydrogen production is examined in this study, the levelized costs of hydrogen are of particular interest. The peculiarity of the LCOH calculation in this work is that there are different sources of electricity with different prices and quantities, as well as different electricity requirements at the site, not all of which are part of the hydrogen production. For example, at some point in time, the electricity purchased from the PPAs may exceed the demand for hydrogen production. However, this surplus can then be used to cover the remaining electricity needs at the site and must not be included into the calculation of LCOH.

In order to determine the LCOH, the time-variable electricity price must first be calculated, which depends on which procurement markets are currently being used for H_2 production. Eqs. (27) to (36) calculate these costs with the case distinction that there is a surplus or a shortage of PPA electricity for H_2 production. First, a distinction can be made between the electricity for H_2 production obtained from PPAs $e^{PPA,H2}$ and the day-ahead market, according to Eqs. (27) to (29). In both cases, a mixed PPA electricity price is initially calculated using Eq. (31) where $C_{PPA,t,s}$ denotes the total costs from PPA procurements in timestep t and scenario s. In the event of a PPA surplus, this PPA price is multiplied by the amount of electricity for hydrogen production and the revenues from resale on the day-ahead market and the theoretical revenues from further use in the company are deducted from this. The theoretical revenues arise because, without the PPA supply, the company would still have to purchase the electricity on the day-ahead market and therefore the price difference between PPA and the day-ahead market is included here as revenue (or loss). In the case of shortage (Eqs. (34)–(35)), the share of electricity for H_2 production is settled with the mixed PPA price. In addition, costs arise from additional day-ahead procurement. In both cases, surplus or shortage of PPA electricity, the total cost are divided by the electricity required for H_2 production e^{H2}. Finally, $c^{H2}_{total,t}$ in Eq. (36) defines the time- and scenario-dependent electricity price for hydrogen production with a case distinction for surplus or shortage situations.

$$e^{H2}_{t,s} = P^{Prod\,H_2}_{t,s} \cdot \Delta t \tag{26}$$

$$e^{PPA}_{t,s} = P^{PPA}_{t} \Delta t \tag{27}$$

$$e^{PPA,H2}_{t,s} = \min(e^{PPA}_{t,s}, e^{H2}_{t,s}) \tag{28}$$

$$e^{DA,H2}_{t,s} = e^{H2}_{t,s} - e^{PPA}_{t,s} \tag{29}$$

$$e^{sell,DA}_{t,s} = P^{DA,Sell}_{t,s} \cdot \Delta t \tag{30}$$

$$c_{PPA,t,s} = \frac{C_{PPA,t,s}}{e^{PPA,H2}_{t,s}} \tag{31}$$

$$\begin{aligned} C^{surplus}_{elec,t,s} = {} & e_{H2} \cdot c_{PPA} \\ & - (e_{PPA,t} - e_{H2,t} - e^{sell}_{DA,t}) \cdot (c_{DA,t} - c_{PPA}) \\ & - e^{sell,DA}_{t,s} \cdot (p^{DA}_{t,s} - c_{tr}) \end{aligned} \tag{32}$$

$$c^{surplus}_{elec,t} = \frac{C^{surplus}_{elec,t}}{e_{H2,t}} \tag{33}$$

$$C^{shortage}_{elec,t} = e_{PPA,H2,t} \cdot c_{PPA} + e_{DA,H2,t} \cdot c_{DA,t} \tag{34}$$

$$c^{shortage}_{elec,t} = \frac{C^{shortage}_{elec,t}}{e_{H2,t}} \tag{35}$$

$$c^{H2}_{total,t} = \begin{cases} c^{shortage}_{elec,t} & ;\text{if } e_{PPA,t} \le e_{H2,t} \\ c^{surplus}_{elec,t} & ;\text{else} \end{cases} \tag{36}$$

The LCOH can be calculated using Eq. (37) with the electricity prices calculated above. On the cost side, the annual investment costs according to Eq. (22), the electricity costs for hydrogen production and the costs for the transformer expansion due to the peak load increase are incurred. These costs are divided by the total annual amount of hydrogen produced m_{H2}.

$$LCOH = \frac{C^{CAPEX} + \sum_{t\in T} e_{H2,t} \cdot c^{H2}_{total,t} + C^{PeakIncrease}}{m_{H2}} \tag{37}$$

As described above, it makes sense to take the levelized costs for the total electricity supply into consideration, since there are also electricity purchases other than those for hydrogen production. The LCOE takes into account CAPEX (see Eq. (22)), the cost of purchasing electricity, revenues from sales on the day-ahead market and costs from peak load increase. All costs are divided by the electricity demand for hydrogen production as well as other electricity demands of the company (see Eq. (38)).

$$LCOE = \frac{C^{CAPEX} + C^{DA} + C^{PPA} + C^{PeakIncrease}}{\Delta t \cdot \sum_{t\in T} P^{import}_{t} / \eta_{Traf}} \tag{38}$$

2.4.2. Ecological parameters

CO_2 emissions are a frequently considered indicator of the ecological impact of an energy system. For this purpose, the purchases from PPAs are considered CO_2-free, so that the total CO_2 emissions are caused by purchases on the day-ahead market only. The amount of CO_2 emissions per kWh procured electricity from the grid is given through $f_{CO2,t}$ and results in the formulation of Eq. (39).

$$E_{CO2} = \Delta t \sum_{t\in T} f_{CO2,t} \cdot (P^{DA,buy}_{t} - P^{DA,sell}_{t} - P^{curtail}_{t}) \tag{39}$$

The CEF from [18] quantifies the share of zero-emission electricity in total purchases. We consider electricity from PPAs to be renewable. Since RED2 also allows the use of conventional electricity purchases for the production of green hydrogen if it is cheaper than 20 $€_{2024}$ MWh^{-1} [9], this electricity is also considered renewable in the calculation of the CEF with Eq. (40). For this, the binary variable $b_{DA,t}$ has the value 1 if the day-ahead price in hour t is lower than 20 $€_{2024}$ MWh^{-1} and 0 if not.

$$\begin{aligned} CEF = {} & \frac{\Delta t \sum_{t\in T} P^{DA,buy}_{t,s} \cdot b_{DA,t} + P^{PPA}_{t}}{\Delta t \sum_{t\in T} P^{PPA}_{t} + P^{DA,buy}_{t}} \\ & - \frac{P^{DA,sell}_{t} + P^{curtail}_{t}}{\Delta t \sum_{t\in T} P^{PPA}_{t} + P^{DA,buy}_{t}} \end{aligned} \tag{40}$$

3. Case study

This work analyzes a real-world glassworks site in Germany as a potential hydrogen producer where today's NG-fired furnace is replaced by a hydrogen-fired one [5]. We consider a hydrogen production serving this demand through electrolysis on-site. The first section of this chapter explains and parametrizes the energy system model for this case study using the methodology from above (see Section 2). The following section then gives an overview of all analyzed scenarios in this study. We wrote the optimization model to calculate these results in Python [27]. The code is available upon request. We calculated all scenarios using a machine with two AMD EPYC 7H12 64-core processors and 2 TB of RAM. Each scenario was calculated separately, with the runtime increasing to multiple days as the number of available PPA contracts decreased.

3.1. Setup

Fig. 1 provides a schematic overview of the energy system analyzed in this study. The energy system requires parametrization that includes component efficiencies or PPA prices and time-dependent data for RES power factors, wholesale prices and demand data. The model developed in this work creates four scenarios making the optimization more robust to the uncertainty, especially with time-dependent input data. For this,

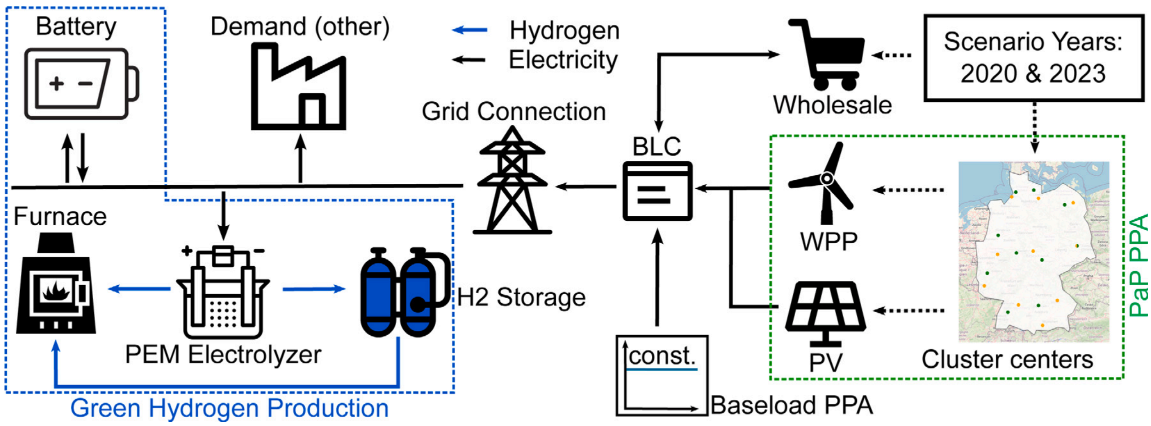

Fig. 1. Schematic representation of the energy system model for the glassworks analyzed in this case study. The company's electricity procurement activity is handled by the balancing circle (BLC).

wholesale prices and power factors from 2020 and 2023 are combined with two hydrogen demand scenarios.

As the glassworks use case of this study is located in Germany, the German hourly day-ahead price is used for wholesale procurement [28]. For the scenario-dependent PPA modeling, locations of weather observation stations from the German Weather Service (DWD) have been used. All stations where irradiance or wind speed observations for both years 2020 and 2023 exist have been considered as possible locations for renewable electricity generators [29]. Our dataset includes 103 observation stations measuring solar radiation for both years. We convert global horizontal irradiance values into power factors using the *Python* package *pvlib* [30]. For wind speed observations, there are 167 stations available. We apply the *windpowerlib* Python package to translate these measurements from the height of 10 meters into power factors based on the reference wind turbine "E126" at 135 meters height [31]. To limit the computational complexity of the stochastic problem, all locations have been clustered with a K-means approach into 10 clusters per generator type. For each cluster, the closest observation station to the centroid is used as a representative station for this cluster. Appendix A.1 lists these representative weather stations and their locations. Finally, for each PV location, four different orientations per site have been modeled by varying the orientation parameter in the *pvlib* power factor calculation. In summary, this study includes 10 power factor timeseries for WPP locations per year and 40 different profiles for PV generators (see Fig. 2).

Hydrogen demand values were obtained from [32] for glass melting furnaces transitioning from natural gas to hydrogen supply. The data originates from 2019 measurements but is expected to be independent of years when a constant production is assumed. The glasswork's hydrogen demand is 5500 t per year for supplying a furnace that has an additional electricity boosting of 8 MW. Including the electrolyzer efficiency, this corresponds to 406 MWh of electricity demand for green hydrogen production. Fig. 3 displays the hydrogen demand in the blue line based on calculations from [33]. The data shows a constant high demand between 19 and 22.5 MW with a high demand plateau in the first half of the year. In order to take into account a possible shift of that plateau in the optimization, a second demand scenario was created in which the time series was shifted by 6 months (yellow line).

In industrial settings, hydrogen is primarily stored in pressure vessels [34]. However, regulatory constraints limit the amount of hydrogen allowed to be stored without any additional safety measures to 5 *t*, as hydrogen is classified as a dangerous substance [35]. Consequently, we establish a maximum capacity limit of 167 MWh for hydrogen storage systems due to these regulations. In Appendix A.2 we provide exemplary results for a scenario without this constraint to find the theoretical optimal sizing of the hydrogen storage.

The electrolyzer can be seized to up to 60 MW. We model a PEM electrolyzer with a static efficiency. In order to take into account non-modeled influencing factors such as maintenance work, ramp-up phases and aging, a conservative system efficiency of 45.6% is assumed in this work. Table 1 summarized all relevant parameters for this case study.

Pricing PPA contracts depend on site and contracts specific parameters like producer margins, durations or generator types [11]. This study assumes values from [13] for the contract types from PV generators or WPP. The estimated cost of baseload PPAs is 200 $€_{2024}$ MWh^{-1}. It is important to acknowledge that a baseload PPA generally necessitates the inclusion of electricity from hydroelectric power plants, as these sources are consistently available. Furthermore, the location of these power plants must be within Germany, in accordance with the provisions outlined in the RED2 regulations. In addition, the age of the plants must not exceed 36 months. Given the complexity of implementing such a power supply in Germany, the price is expected to increase, reflecting the limited availability of the commodity.

The years for day-ahead market prices match the weather year. Thus, we use the 2020 and 2023 hourly prices for two scenarios each with average values of 30.4 $€_{2020}$ MWh^{-1} and 95.2 $€_{2023}$ MWh^{-1}, respectively. We assume that the electricity demand for green hydrogen production is free from levies. Therefore, only the remaining electricity demand on site, which is fixed in every scenario, is subject to levies. To better generalize the calculation, we exclude these levies. The grid emission data, however, is used only from the year 2023 as the generator mix in Germany considerably changed since 2020 and the emission data from 2020 does not represent future scenarios anymore. On average, day-ahead procured electricity comes with 308.9 g kWh^{-1} CO_2 emissions [36].

The generated power in the RES faces losses from inverting and transforming the electricity at the generator's site. Additionally, transmission losses occur. The average distance to all cluster locations is 373 km. Assuming a loss of 3% per 500 km [37], this leads to a mean distribution loss of 2.42% for this study. Including 4% losses for inverters and transformers at the generation site [38], it adds up to 6.3% total losses from the RES to the off-takers grid access point. The battery system is modeled including an inverter. We assume the battery to have a E2P ratio of 4 as there is a trend towards higher-hour systems in Germany especially with batteries that are being used in multiple stacked applications. With this E2P ratio, the total system costs add up to 263.5 $€_{2024}$ kWh^{-1}

3.2. Scenarios

To analyze the effect of portfolio optimization, this study examines different portfolio limits b^{PPA}_{max} that specify the maximum number of PaP contracts an off-taker can close. Moreover, the use of battery

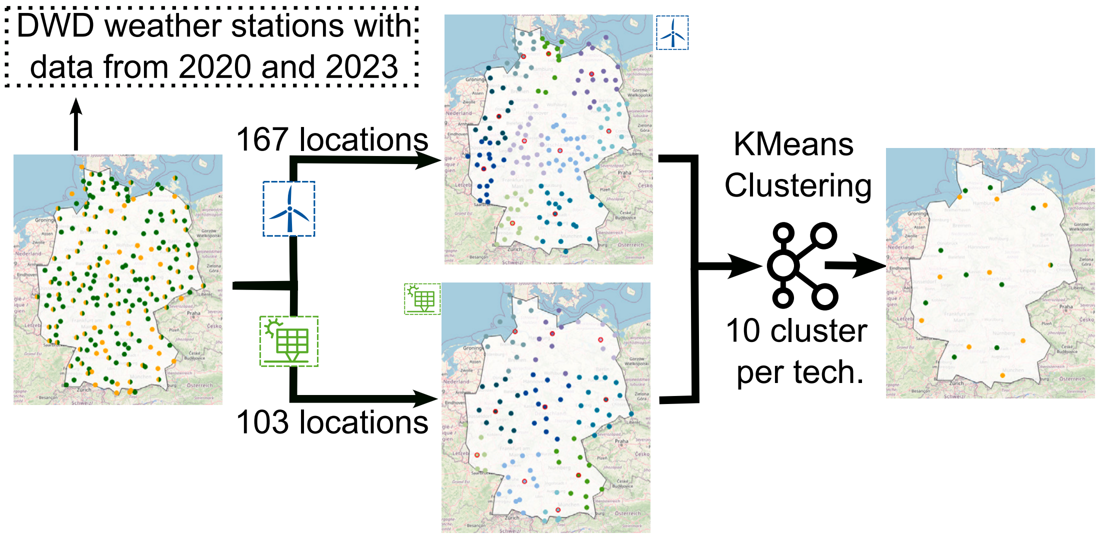

Fig. 2. Clustering process for representative electricity generation profile: First, raw data from German Weather Service (DWD) with available data for the years 2020 and 2023 is extracted. Then, all locations for each technology are clustered into 10 clusters using the K-means technique where the observation locations closest to the center represent each cluster.

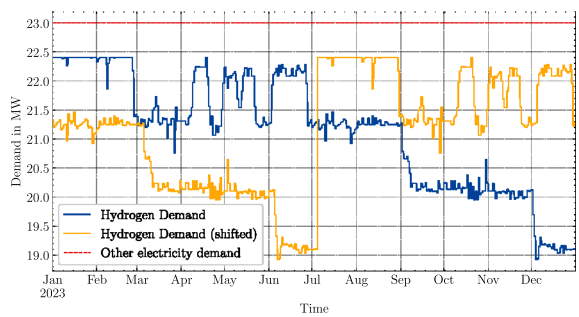

Fig. 3. Hydrogen demand of the analyzed glasswork. The original data from [33] in blue and the shifted scenario in yellow. The original measurement has been done in 2019. The red curve illustrates a theoretical constant electricity demand of the company outside of the hydrogen production.

storage and different matching regulations are examined. For electricity procurement without matching requirements and PPA contracts, only day-ahead market access is defined as the benchmark scenario for the analysis.

The first scenario class includes the RED2-compliant scenarios, which analyze the scenarios under the hourly adjustment scheme that takes place from 2030 onwards. The reference scenarios "RED2-reference" include a battery storage and up to 50 allowed contracts for the glasswork. The "No-BAT" scenario compares the RED2-reference to a scenario without battery storage installation. Uncertainty still exists in the first two scenarios regarding the prices of baseload and PaP contracts. Thus, a parameter study of baseload prices (RED2-Baseload) and PaP prices for PV and wind PPAs (RED2-PaP) has been conducted. In these scenarios, the prices for contracts vary but the rest of the parametrization in Table 1 stays the same.

Finally, to analyze the effect of different temporal matching schemes, the scenarios "Yearly", "Monthly", "Weekly" and "Daily" can be compared against the RED2-Reference scenarios. Each is using the parametrization of Table 1. All scenarios are summarized in Table 2.

Table 1
Parameter settings for the case study.

Param.	Val.	Unit	Ref.
PPA			
PV price	53	€$_{2024}$ MWh^{-1}	[13]
WPP price	57	€$_{2024}$ MWh^{-1}	[13]
Baseline price	200	€$_{2024}$ MWh^{-1}	Assump.
Losses (Inv. & Trans.)	4	%	[38]
Dist. losses	2.42	%	[37]
Battery			
Battery costs	243	€$_{2024}$ kWh^{-1}	[39,40]
Inverter costs	82	€$_{2024}$ kW^{-1}	[39]
Battery eff. (1-way)	98	%	[38]
Inverter eff. (1-way)	97	%	[38,41]
E2P ratio	4	/	Assump.
Lifetime	20	years	[39]
Hydrogen			
Electrolyzer costs	1643	€$_{2024}$ kW^{-1}	[42]
Electrolyzer eff.	45.6	%	[43,44]
H_2 storage costs	25.7	€$_{2024}$ MWh$^{-1}_{H2}$	[45]
H_2 storage eff. (CHA)	91	%	[46,47]
E2P H_2 storage	40	/	Assump.
Financials			
Inv. horizon	20	a	[48]
WACC	8.5	%	[49]
Infl. rate (10-year avg.)	1.354	%	[50]
Max. Sell/Demand ratio	20	%	[18]
Other			
CO_2 emissions	Avg: 308.9	g/kWh	[36]
DA prices	Avg 2020: 30.5	€$_{2020}$ MWh^{-1}	[51]
	Avg 2023: 30.5	€$_{2024}$ MWh^{-1}	[51]

4. Results

This section shows the results for the glassworks presented in Section 3. In the first part, we analyze all scenarios under current RED2 compliant settings with hourly matching with an hourly matching scheme. We compare the influence of adding the battery storage on-site and investigate the prices of PPAs with a parameter study. The second section focuses on alternative matching schemes and their influence on economic and ecological performance indicators.

4.1. Portfolio optimization & battery usage

In the pursuit of optimizing baseload energy reduction, achievements can be made through the optimization of PPA portfolios as can

Table 2
Scenario overview for transitioning the energy system of the glassworks case study to a hydrogen-based glass furnace.

Name	Parameters					
				PPA Prices in €$_{2024}$ MWh^{-1}		
	RES Limit	Matching Scheme	Battery included	Baseload	PV	Wind
Benchmark	Only day-ahead market procurement					
RED2-compliant scenarios						
Reference	0–50	Hourly	✓	200	53	57
No-BAT	50	Hourly	x	200	53	57
Baseload	12	Hourly	✓	100–300	53	57
PaP	12	Hourly	✓	200	40–100	40–100
Temporal Matching						
Daily	0–50	Daily	✓	200	53	57
Weekly	0–50	Weekly	✓	200	53	57
Monthly	0–50	Monthly	✓	200	53	57
Yearly	0–50	Yearly	✓	200	53	57

be seen in Fig. 4. The figure shows the amount of energy purchased by the company in the RED2-reference scenario from each source without using a battery storage (left bars) and with battery (right bars). The red lines on the second y-axis display the need for baseload energy compared to the portfolio with only one allowed PPA contract without battery usage. Without using the battery, even in the case of the largest portfolio, the baseload consumption can only be reduced by around 6%. It is also notable that this reduction is already achieved with 2 PaP contracts. Closing more than these two contracts without battery storage is not viable for the glassworks in this scenario. Similarly, the results in Figure show for the portfolios with battery storage that portfolios larger than 10 contracts do not bring any more significant baseload consumption decrease. Therefore, it is important to emphasize that the optimizer will not use all available contracts in all scenarios if they do not bring added value. The number of contracted generators can be seen in Table A.4. With only one allowed PaP contract, the optimizer favors wind over PV generation with an optimal amount of purchased electricity of 248 GWh. By combining several contracts, PV generation in particular is added due to the lower costs. In the case of the largest portfolio around 140 GWh is purchased from WPP and 150 GWh from PV systems, which corresponds to a PaP share of around 40%. The amount of electricity from the DA market reduces from 105 GWh when only one PaP PPA is used to 89.9 GWh for the largest portfolio.

By adding the battery storage, the baseload purchases can be reduced as it represents the most expensive electricity import option. In the case of the largest portfolio a reduction by up to 26% takes place. In addition, just over 403 GWh of PaP electricity is purchased, which corresponds to 33% more than in the case without the battery. The PaP share of total electricity purchased rises to 54%. Another difference to the result without the battery is that the purchase of energy from WPPs is almost three times as large as the PV purchase. Due to the continuous generation profile of wind turbines, this technology is best suited to replace expensive baseload energy. However, without the battery storage system, the results show that this is only possible to a limited extent. Adding the battery storage lowers day-ahead procurement for multi-PPA portfolios. In case of 50 allowed contracts, the amount decreases from 89.9 to 68.9 GWh.

In two cases (3 allowed contracts without battery and 9 allowed contracts with battery) the baseload imports increase even though the number of allowed contracts rises. This can be explained with the optimization's optimality gap of 2%. The overall objective change from the increase in baseload contract volume is lower than this gap. This means that the optimizer could not find a significantly better solution with the larger portfolio by using the extra PaP PPA.

Finally, it can be seen that the total amount of electricity purchased does not substantially increase as a result of the portfolio expansion. By adding the battery, an additional amount of electricity is purchased, which is associated with losses when the battery is used.

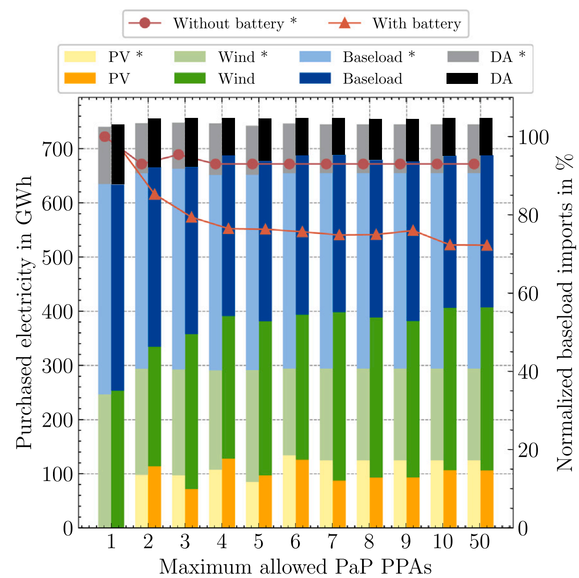

Fig. 4. Impact of PPA limits on bought electricity and baseload PPA imports. The stacked bars represent energy sources: PV (yellow), WPP (green), baseload (blue), and day-ahead market (black). Left bars marked with "*" show results for scenarios without battery storage.

Next, Fig. 5 shows how the portfolio sizing influences the components' dimensions for the scenarios considering battery installation. The maximum average contract size for PV and WPP is reached at over 160 MW when only one or two contracts are allowed. With three contracts permitted, the average sizes remain similar for both generators with approximately 85.7 MW for PV and 84.4 MW for WPP. In scenarios with larger portfolios, there is potential to significantly reduce these average sizes down to less than 16.7 MW for PV generators and 33.1 MW for WPPs. Consequently, baseload power decreases from an initial level of 50.2 MW with one PPA to over 40 MW with three PPAs and eventually settles at around 32.4 MW with 12 allowed PPAs.

The dimensioning of the battery storage correlates with the dependency on baseload contracts. As soon as more than 1 PPA is contracted and thus the baseload requirement falls by 15%, the battery size jumps to more than 160 MWh. As the portfolio grows, the baseload dependency is only slightly reduced and the battery dimensioning remains largely between 150 and 160 MWh. In the portfolio with 9 PPA contracts as a limit, the optimization has purchased a larger share of baseload energy, which in turn leads to a smaller storage dimensioning of still 95.4 MWh.

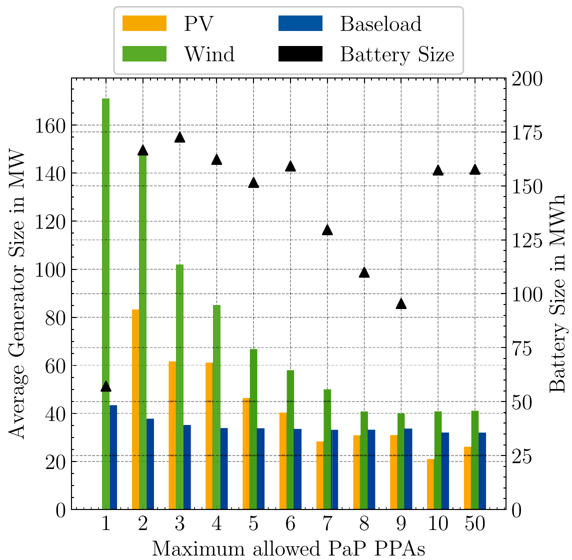

Fig. 5. Average contract size for different portfolio sizes and battery capacity on the right axis.

The results for the reference scenarios demonstrate that battery optimization in conjunction with PPA portfolio optimization enhances efficiency in achieving substantial reductions in required baseload levels. Storage and PPA portfolio do not serve as a replacement for the other, but rather as a complement, cooperatively contributing to reducing the demand of baseload power.

The selection of locations for the PPA generators is essential, as the generation profiles and quantities per installed capacity vary widely in Germany. Typically, the north has a significantly higher load factor for wind turbines, whereas PV systems are utilized more in the south of Germany. In addition, an east-facing PV system, for example, can generate more energy in the morning hours than a west-facing PV system. Fig. 6 shows how the geographical distribution changes with the portfolio size and battery utilization. Comparing the smallest possible portfolio with one allowed contract in the left with the portfolio where 50 contracts are allowed (center) shows the diversification of the portfolio towards several small systems spread across Germany. The average system size decreases from 167 MW with one WPP contract to 24 MW for WPPs and 29 MW for PV systems for the large portfolio, where 8 generators are contracted in total. Adding a battery to the portfolio (right) makes it beneficial to add even more contracts to the portfolio. Here, the WPPs and PV generators have an average size of 33 MW and 20 MW, respectively.

If only one PPA contract is allowed, the optimization selects a wind turbine in southern Germany (ID 10 in Table A.3) with an average capacity utilization of 1481 full-load hours across all 4 scenarios considered in the stochastic optimization. This is not unusually high for wind turbines. At other locations included, up to 3000 h can be achieved. Fig. 7 compares the undersupply of PaP electricity from the selected plant in the south with a better-utilized plant in the north of Germany with 3000 full-load hours. For this comparison, the plant in the north was dimensioned to generate the same amount of electricity as the plant in the south, which corresponds to an electrical power rating of 82 MW.

Two main characteristics can be observed. First of all, the total undersupply in the case of the selected plant in the south is around 10% higher than in the case of the plant in the north. However, since the baseload PPA must be dimensioned in such a way that PPA electricity is available at every hour of the year, it is not the sum of the undersupply that is relevant, but the maximum undersupply that occurs (see Fig. 7, X=0). The maximum undersupply for the PPA site in the south is about 5 MW lower than for the location in the north. With the assumed baseload price of 200 $€_{2024}$ MWh^{-1}, reducing the baseload contract by 5 MW alone would lead to savings of 8.76 Mio. $€_{2024}$. Finally, the following analyzes the influence of battery and portfolio sizing on the total hydrogen production costs. Fig. 8 shows the LCOH for the scenarios without battery (left bars) and with battery (right bars). The dashed line shows a benchmark LCOH value for the theoretical case in which hydrogen is produced directly from conventional grid electricity regardless of simultaneity. Buying all electricity on the DA market results in LCOH of 6.17 $€_{2024}$ kg^{-1}. The LCOH values for the green hydrogen production with hourly matching are significantly higher for all portfolios. However, both approaches, with and without battery, show potential savings through portfolio optimization. With this optimization, the LCOH can be reduced by 6.24% from 15.22 to 14.3 $€_{2024}$ kg^{-1} without battery installation. This cost level is already achieved with relatively small portfolio sizes with two allowed PaP contracts. When the hydrogen producer installs a battery storage, the LCOH can be reduced to 11.8 $€_{2024}$ kg^{-1}. This reduction requires the contracting of larger portfolios with at least 8 allowed PaP PPAs.

4.2. PPA price variation

The biggest uncertainty derives from PPA pricing. Thus Figs. 9(a) and 9(b) show the LCOH for different PPA prices.

In Fig. 9(a) the baseload prices range from 100 to 300 $€_{2024}$ MWh^{-1} while the PaP PPA prices do not change. With baseload costs of 100 $€_{2024}$ MWh^{-1}, which is close to the level of average day-ahead prices in Germany of 95.18 $€_{2024}$ MWh^{-1}, the LCOH is at 6.17 $€_{2024}$ kg^{-1}. For the highest baseload costs of 300 $€_{2024}$ MWh^{-1} it increases to 12.55 $€_{2024}$ kg^{-1}. At the same time, the battery sizes increase with the baseload costs from 33.5 MWh with the lowest baseload contract price to up to 431 MWh. This is because it becomes financially more attractive to reduce the baseload imports with higher prices. The hydrogen storage size, which is not shown in the figure, has been dimensioned to the maximum allowed size of 167 MWh in all cases due to its low installation costs. Fig. 9(b) shows the LCOH resulting from different prices for PV and Wind PPAs and 9(c) illustrates the corresponding battery sizings for these scenarios. In contrast to the baseload variations, the battery sizes increase with lower PaP contract prices. With lower prices for electricity from PV generators and WPPs, it becomes financially attractive to buy more volatile energy and intermediately store it in the battery. This leads to battery sizings of up to 222 MWh for the lowest price combination. With higher PaP PPA prices, the optimal battery size decreases to 60 MWh as it becomes increasingly unattractive to temporarily store the variable PPA energy. However, even for the combination of lowest PaP PPA prices for PV and WPP electricity, the LCOH only reduces to 8.9 $€_{2024}$ kg^{-1}, which is almost 50% higher than the LCOH without matching regulations.

Overall, the variation of price parameters shows the financial challenge facing hydrogen producers. On the one hand, the LCOH values are significantly higher for most scenarios compared to the benchmark with only DA market procurement. On the other hand, the results illustrate the strong influence of PPA pricing on the producer's financial results.

4.3. Temporal matching

The subsequent chapter will examine the impact of less stringent simultaneity rules on carbon emissions and the share of renewable energy on the costs of hydrogen production. To this end, the results of the reference scenario will be compared with those of the theoretical alternative temporal matching scenarios (see Section 3.2). Fig. 10 shows the LCOH for all of the different temporal matching schemes considered for the hydrogen production and allowed PPA portfolio sizes. The gray line indicates the LCOH of 6.21 $€_{2024}$ kg^{-1} for the benchmark scenario where all electricity is purchased from the day-ahead market. There are fundamental differences between the respective schemes. The loosening to daily matching reduces the costs only slightly for all portfolios.

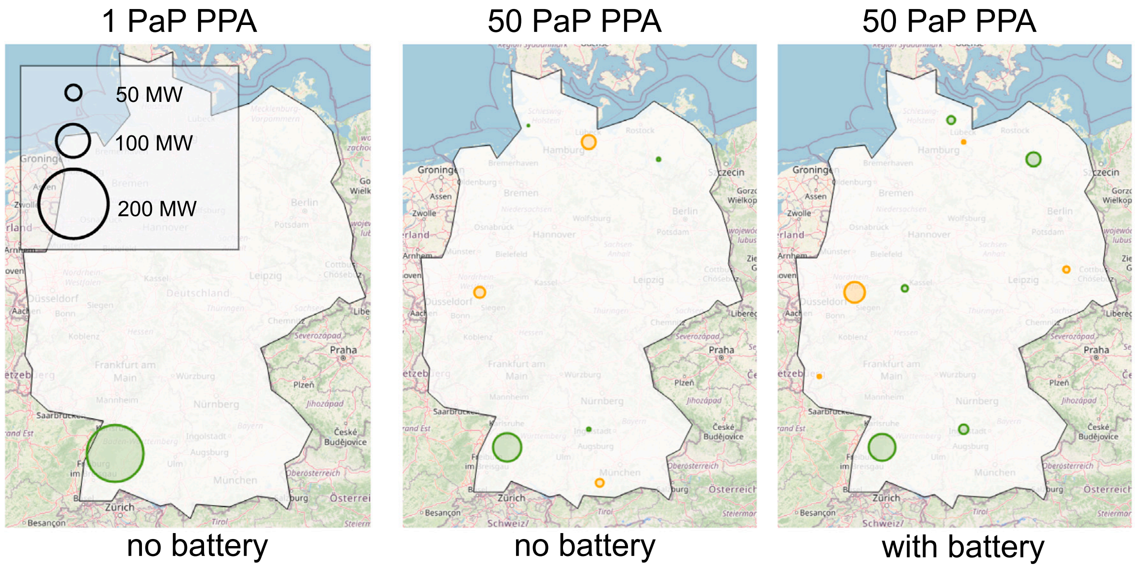

Fig. 6. Locations of contracted PPA generators for different maximum allowed PaP PPAs. Yellow circles show PV generators and green circles WPPs. The circle size corresponds with the contract size of each generator.

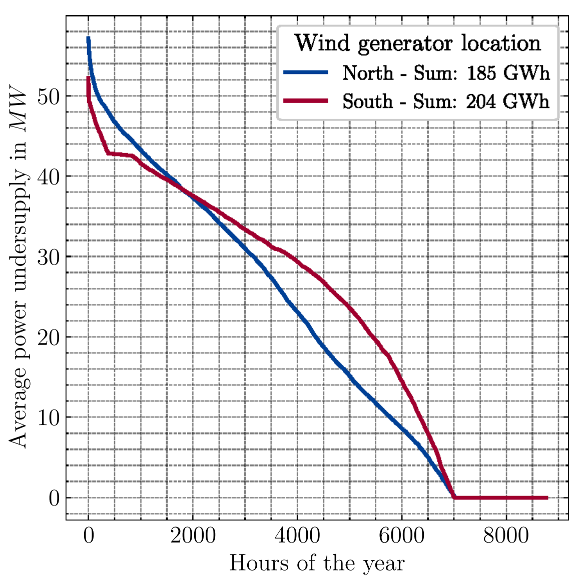

Fig. 7. Comparison of two WPP locations. The one chosen by the optimization in the south (ID 10 from Table A.3, red line) is compared to the WPP with the highest electricity generation (blue) from all observations which is located in the north.

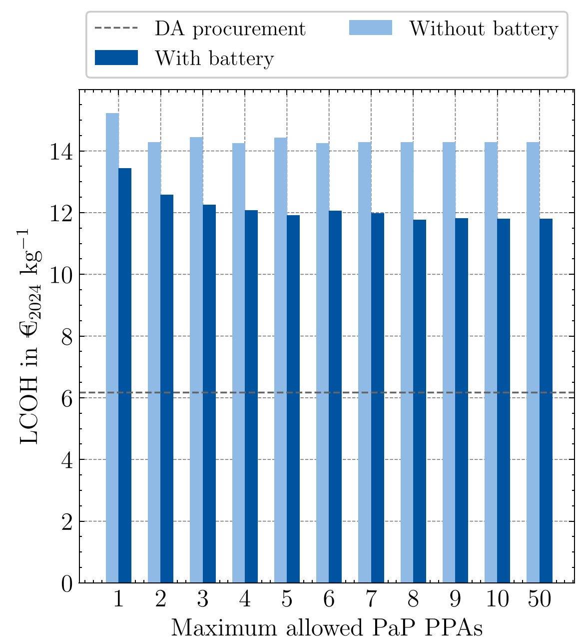

Fig. 8. LCOH for the varying maximum allowed PaP PPAs in the portfolio of the glassworks with (dark blue) and without (light blue) BESS usage. The dotted line depicts the costs if all electricity would be bought on the day-ahead market without matching regulation.

Weekly matching can reduce costs already by almost 2 $€_{2024}$ kg^{-1}. With monthly and annual matching, the LCOH reduces substantially to as low as 4.82 $€_{2024}$ kg^{-1}. On the contrary, the highest LCOH are for the hourly scheme, where even with the largest portfolio the LCOH is still 11.8 $€_{2024}$ kg^{-1}. The different matching rules also lead to different reduction potentials through portfolio optimization. For instance, with annual matching, the LCOH is reduced by 2% compared to the use of just one PaP PPA. The largest reduction is possible in the case of weekly matching, where a decrease of 24% is achieved. In the other cases it is around 12%–14%.

However, it should be noted that the objective function of the optimization model targets an overall cost reduction which besides hydrogen production also includes other electricity consumption of the industrial site considered. Therefore, Fig. 11 shows the LCOE for all electricity purchased at the site. Although this reveals that monthly and annual matching leads to significantly lower costs than the other schemes, the difference is smaller compared to the LCOH results. The LCOE for hourly matching is about 85% higher than for monthly matching, depending on the size of the portfolio. The cost difference is reduced compared to the LCOH as surpluses from PaP procurement can be used to cover other power demands of the industrial site, allowing cheaper electricity to be reused that would otherwise have had to be

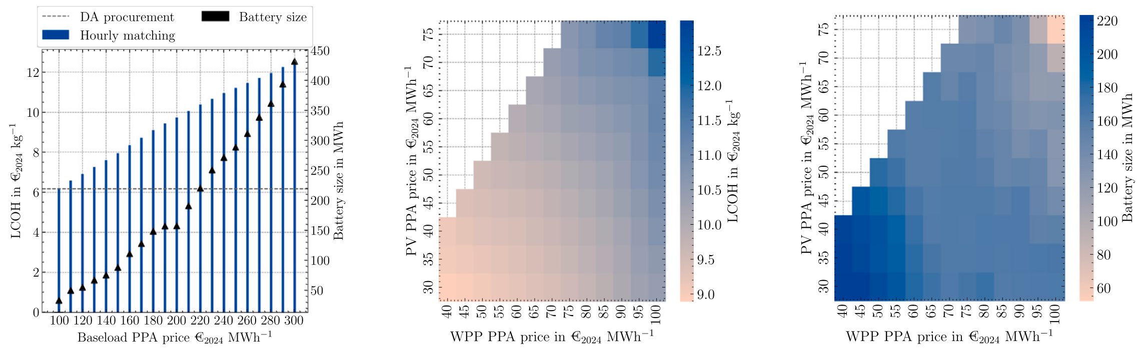

(a) LCOH for different baseload PPA prices.

(b) LCOH for different PaP PPA price combinations.

(c) Battery sizing for different PaP PPA price combinations.

Fig. 9. Sensitivity analysis for RED2 compliant scenarios and hourly matching.

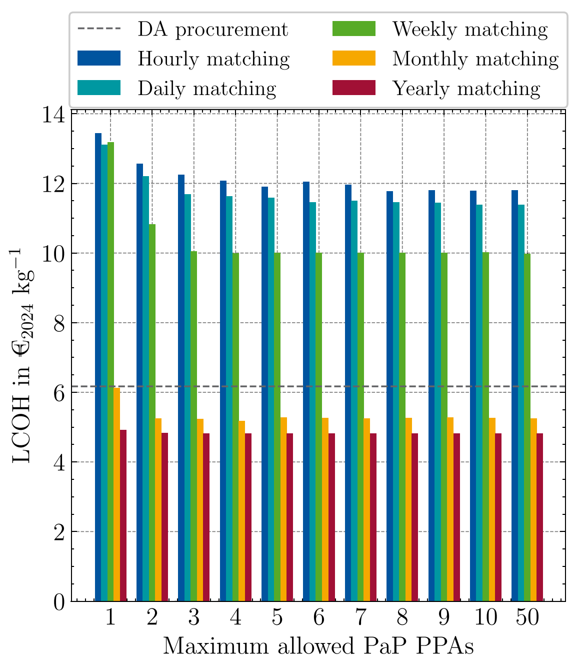

Fig. 10. Levelized cost of hydrogen (LCOH) depending on the matching scheme and allowed number of PaP PPA contracts to be closed. The dotted line shows the LCOH for electricity procurement exclusively via day-ahead market.

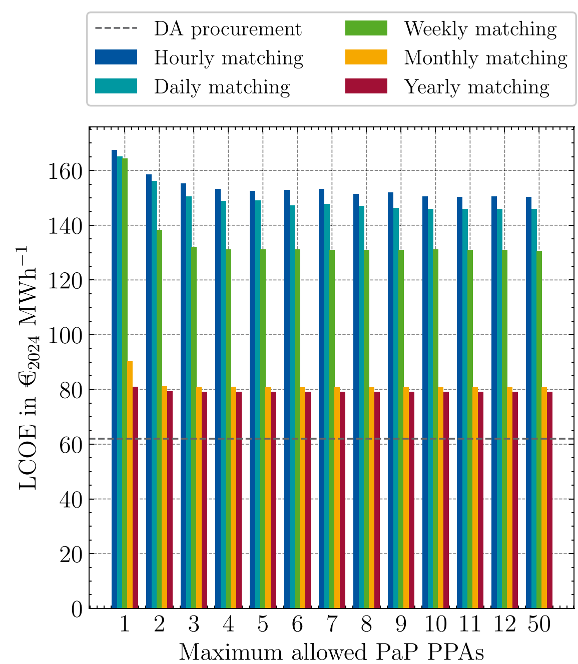

Fig. 11. Levelized cost of electricity (LCOE) for the whole modeled energy system depending on the portfolio size and matching scheme. The dotted line shows the LCOE for electricity procurement exclusively via day-ahead market.

sold. This cost-saving is not included in the calculation of the LCOH. For the portfolios with a maximum number of allowed PPA contracts, the LCOE is 150 $€_{2024}$ kWh^{-1} for hourly matching and 80 $€_{2024}$ kWh^{-1} for monthly matching, which is considerably above the 63 $€_{2024}$ kWh^{-1} in the benchmark scenario without PPAs.

Another important question to analyze is how much green electricity is used if less stringent matching schemes are used. Two indicators are considered in the following. Firstly, this includes the Clean Energy Factor (CFE), which shows the percentage of renewable electricity consumed. Secondly, we consider the CO_2 emissions in the purchased electricity. The results are shown in Figs. 12 and 13.

Fig. 12 illustrates the shares of renewable energy in electricity for hydrogen production (blue) and for total electricity consumption including the remaining electricity demand at the site (red) for the different matching schemes. The gray dashed line indicates the factor for the benchmark scenario, which is 59%. In the case of hourly matching, completely renewable electricity is used for hydrogen production. The share for matching the total electricity demand with green electricity is similarly high at 95%, which is because surpluses from the PPAs can also be used for this electricity demand. The share decreases with the less stringent matching rules. With weekly matching, 94% of the electricity for hydrogen production is still of renewable origin. For monthly and annual matching, on the other hand, only 81% and 75% of the demand for hydrogen production is covered by green electricity.

Fig. 13 displays the annual CO_2 emissions for different portfolio sizes and matching schemes. The gray line depicts the emissions of the benchmark scenario of 192 *kt* per year. It can be seen that all PPA scenarios lead to significantly lower CO_2 emissions. Even with annual matching and only one PaP PPA, emissions can be reduced by 36% compared to pure day-ahead procurement. There is also a significant reduction potential when switching from monthly matching to tighter

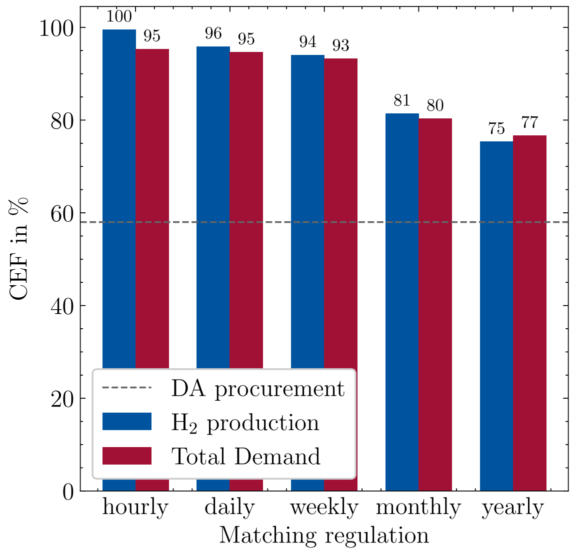

Fig. 12. Clean energy factor (CEF) for different temporal matching regulations considering the electricity used to supply the whole glassworks (red) or only the one for H_2 production (blue). The dotted line shows the CEF for the benchmark scenario where all electricity is procured on the day-ahead market.

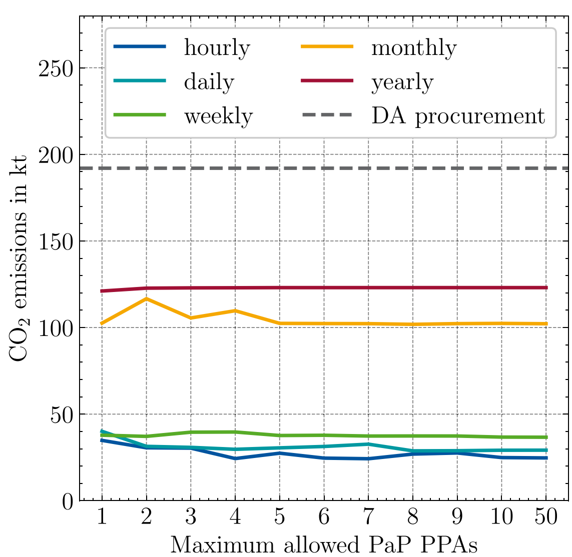

Fig. 13. The glassworks CO_2 emissions from electricity procurement.

regulation. In all scenarios with weekly or stricter schemes, emissions are at least 80% lower than in the benchmark scenario. It can also be observed that stricter regulation enables PPA procurement to further reduce CO_2 emissions, whereas emissions remain constant across all portfolios with monthly or annual matching. As a result, emissions can be reduced by 29% from an initial 34.8 *kt* CO_2 emissions to 24.7 *kt* per year with the largest allowed PPA portfolio in the case of hourly matching.

In summary, the findings indicate that the matching regulation exerts a substantial influence on all KPIs. We observe lower LCOH for the monthly matching than in the benchmark scenario and up to 45% compared to hourly matching. Compared to the benchmark, CO_2 emissions have the potential to be reduced by 80% with monthly matching. Strict regulation can further mitigate emissions the share of renewable electricity in electricity purchases, but this is accompanied by LCOH increases of up to 125%. A comparison of the LCOE for the total electricity purchased at the site reveals that the disparity remains significant, particularly in the context of hourly matching. This prompts the inquiry into the necessity of hourly matching and the potential benefits of transitioning to weekly matching to achieve a substantial reduction in LCOH while maintaining a comparable utilization of green electricity, not only for hydrogen production but particularly for the site's overall electricity demand.

5. Conclusion

In this study, a stochastic optimization model was employed to investigate the impact of Power Purchase Agreement (PPA) portfolio optimization involving up to 50 different renewable energy sources (RES), the implementation of battery storage, and the effect of simultaneity as per the Renewable Energy Directive II (RED2). This method was applied to a real-world case study of heavy-industry glasswork in Germany. The analysis reveals that both portfolio optimization and battery storage deployment are viable options for influencing electricity procurement for the analyzed use case. Notably, these two strategies do not exclude each other, but rather enhance each other's effectiveness.

The results show that portfolio optimization alone can reduce the levelized cost of hydrogen (LCOH) by up to 6.24% to 14.3 $€_{2024}$ kg^{-1}. The usage of battery storage improves cost reduction through portfolio optimization and can ultimately lead to LCOH of 11.8 $€_{2024}$ kg^{-1}. This cost reduction is primarily driven by a reduced need for baseload PPAs, with portfolio optimization allowing for a reduction in baseload contract size of over 25%. Notably, even a modest number of PPAs can achieve a substantial portion of the total reduction potential so that already 3 contracted RES would reduce dependency on baseload PPAs by over 20%. In portfolios of limited size, the strategic location of generators can be pivotal. This is not merely a matter of observable load at a specific site, but rather, the extent to which it aligns with the unique consumption profile of the company. For instance, a less-utilized generator in the southern region might be better positioned to meet peak demand through PPAs compared to a facility with higher net generation capacity in the north.

The regulatory framework surrounding simultaneity exerts a substantial influence on the outcomes. Strict matching schemes from hourly to monthly simultaneity increase green hydrogen production costs by a minimum of 100% across all portfolios. Loose regulation with monthly and annual matching enables LCOH levels at around 5 $€_{2024}$ kg^{-1}. However, the higher costs associated with stricter regulation in terms of simultaneity result in improved environmental parameters. For example, the CO_2 emissions from grid procurement are doubled in the case of monthly matching compared to hourly matching. The proportion of green electricity in total purchased electricity (CEF) falls to 80% with monthly matching. Already with weekly matching, CO_2 values and CEF can be significantly improved, with considerably lower LCOH than with hourly matching. Looking forward, he observed results of this work aim at providing a foundation for further discussions on whether it makes sense to enforce strict hourly regulation in heavy industry or whether it would be a sensible compromise between costs and ecological benefits to switch to daily or weekly simultaneity.

Future research may involve the expansion of stochastic optimization through the utilization of more sophisticated component models, thereby yielding more precise results. To circumvent protracted computation times, the application of decomposition methods, such as Benders Decomposition, could prove advantageous. The practical implementation of this method may encounter challenges related to PPA-specific pricing, which can be addressed through future code adaptations. A consideration of additional load profiles from other industries could also help to quantify the benefits of PPA optimization

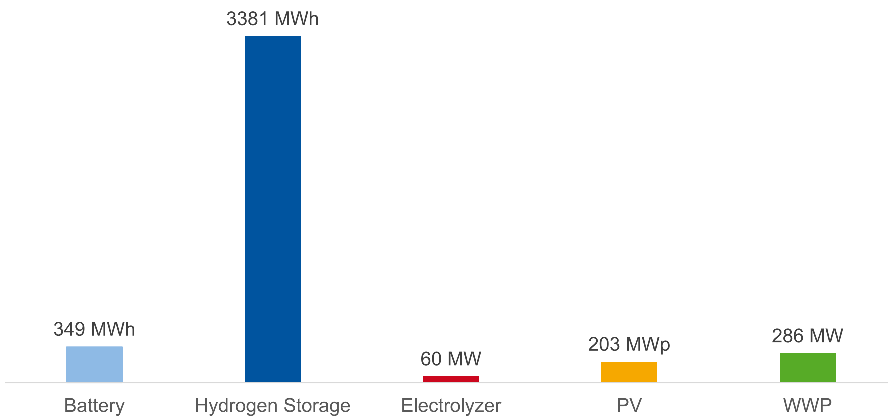

Fig. A.14. Component capacities and PaP PPA sizes per technology when the maximum size of the hydrogen storage is not limited.

more generally. Although only one case study was considered in this work, the methodology applied can be transferred well to other use case. Despite the fact that the code is not yet suitable for commercial use, there are only a few easily adjustable parameters and input values, making it possible for other researchers or engineers to use the program. Finally, the results give a realistic impression of the challenges of future electricity procurement for the production of green hydrogen in general.

CRediT authorship contribution statement

Jonas Bruckscn: Writing–original draft, Visualization, Software, Methodology, Investigation, Data curation, Conceptualization. **Jonas van Ouwerkerk:** Writing–review & editing, Supervision, Methodology, Funding acquisition. **Dirk Uwe Sauer:** Writing–review & editing, Supervision, Methodology, Funding acquisition, Conceptualization.

Declaration of competing interest

The authors declare that they have no known competing financial interests or personal relationships that could have appeared to influence the work reported in this paper.

Acknowledgments

We gratefully acknowledge the funding by the Ministry of Economic Affairs, Industry, Climate Action and Energy of the State North-Rhine Westphalia, Germany (Grant number: EFO 0133E).

Appendix

A.1. Cluster locations

We use data from Deutscher Wetterdienst DWD) [29] for calculating the generated electricity in RES. All weather observation stations with data from 2020 and 2023 have been used and clustered into 10 clusters per technology. For each cluster, we chose the observation station closest to the center as the representative location. Table A.3 lists the cluster representing weather stations with their coordinates.

A.2. Unlimited hydrogen storage

This section shows exemplary results without limiting the size of the hydrogen storage to 167 MWh as in the results above. Fig. A.14 shows the optimized capacities for the battery, the hydrogen storage, and the electrolyzer for the RES-Reference scenario and 50 allowed PaP PPAs. It also shows how much RES power has been contracted for PV generators and WPPs. The hydrogen storage in this scenario has a capacity of 3381 MWh while the battery size increases from 158 MWh with hydrogen storage limitation to 349 MWh.

The overall storage capacity is beneficial to get more independent from the expensive baseload contracts. Fig. A.15 depicts the energy level of the hydrogen storage in the four scenarios of the stochastic optimization problem. Scenarios 1 and 2 use price and weather information from 2020 combined with the original hydrogen demand (blue) and shifted hydrogen demand(turquoise), respectively. Scenarios

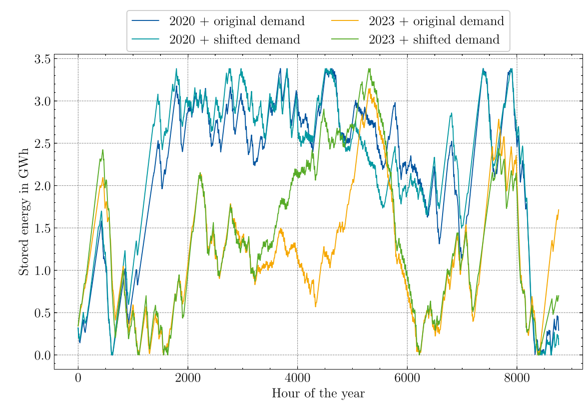

Fig. A.15. Energy level of the hydrogen storage in all four scenarios of the stochastic optimization program. Price and weather information from 2020 and 2023 has been used. These two scenarios are combined with two hydrogen demand scenarios.

Table A.3
List of the cluster representing weather observation stations with their coordinates.

ID	Wind		PV	
	Latitude	Longitude	Latitude	Longitude
1	50.3602	6.8697	51.3932	10.3123
2	50.9829	10.9608	48.8281	9.2000
3	52.1344	7.6969	51.2452	7.6425
4	54.0691	9.0105	53.8713	8.7060
5	48.7918	10.7062	51.6451	13.5747
6	51.6451	13.5747	47.8009	11.0108
7	53.5196	12.6654	53.8025	10.6989
8	51.3219	9.0558	53.5998	13.3039
9	54.1654	10.3519	49.0425	12.1019
10	48.4538	8.4090	49.7479	6.6583

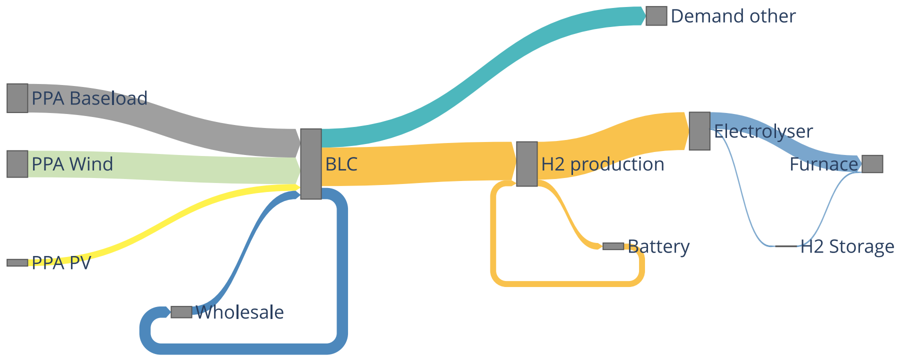

Fig. A.16. Energy flows in the modeled energy system.

Table A.4
Limit for PaP PPA usage and contracted number of PaP PPAs.

Limit of PPA contracts	Contracted PaP PPAs					
	Hourly No Battery	Hourly	Daily	Weekly	Monthly	Yearly
1	1	1	1	1	1	1
2	2	2	2	2	2	2
3	3	3	3	3	3	3
4	3	4		4	4	4
5	5	5	4	5	5	5
6	6	6	5	5	6	5
7	7	7	7	7	6	5
8	7	8	7	6	6	5
9	7	8	8	7	6	5
10	7	10	10	7	6	5
50	7	9	10	7	6	5

3 and 4 use the data from 2023. The usage of hydrogen storage changes with the weather scenario rather than with the demand scenario. This indicates that the generation from PPAs availability is crucial for sizing the hydrogen storage. Both weather scenarios seem to have critical time frames in which the full storage capacity has to be used. In the case of the year 2020, this happens in the hours 8000 to 8400 and in 2023 from hour 5400 to 6200.

The battery storage capacity increases as well but rather for storing the PPA surplus on a daily basis. In the 4 scenarios the battery storage cycles between 303 and 307 times per year.

A.3. Number of contracts in PPA portfolios

Table A.4 shows how many PaP PPA contracts have been used by the optimizer as it is not always necessary to use all available contracts.

A.4. Energy flows for green hydrogen production

Fig. A.16 visualizes the energy flows in the energy system with 50 allowed PaP contracts. The graph illustrates how electricity imports from various sources are utilized. The company's balancing group (BLC) must supply the two consumption channels for hydrogen production (orange) and the remaining electricity demand (turquoise). According to RED2 guidelines, the PPAs only have to be purchased for hydrogen production. In times of surpluses, these can then be used to supply the remaining demand instead of electricity purchased on the market. Further surpluses are sold on the day-ahead market (light blue). Supplying the remaining electricity demand with surplus PPAs can have two advantages: (1) There can be price advantages compared to supplying this demand via the day-ahead market; (2) The quota of renewable electricity for the entire company is increased (more on this in Section 4.3).

Data availability

Data will be made available on request.

References

[1] Schmidt H. Entwicklung der spezifischen Treibhausgas-Emissionen des deutschen Strommix in den Jahren 1990 - 2022. Umweltbundesamt; 2023.
[2] Everling M. Dekarbonisierung in der Flachglasindustrie. 2022.
[3] Zier M, Pflugradt N, Stenzel P, Kotzur L, Stolten D. Industrial decarbonization pathways: The example of the German glass industry. Energy Convers Manag: X 2023;17:100336. http://dx.doi.org/10.1016/j.ecmx.2022.100336.
[4] Voglar J, Likozar B. Critical perspective on green hydrogen-based seasonal operation of energy-intensive industry sectors with solid products. Int J Hydrog Energy 2024;93:910–24. http://dx.doi.org/10.1016/j.ijhydene.2024.11.018.
[5] Institute for Power Generation and Storage Systems. COSiMa Project. 2022, https://www.pgs.eonerc.rwth-aachen.de/cms/e-on-erc-pgs/forschung/projekte/~bfvybd/cosima/?lidx=1.
[6] H2Glass. H2Glass. 2024, https://h2-glass.eu.
[7] Schott. Premiere: SCHOTT produziert optisches Glas mit 100 Prozent Wasserstoff. 2024, https://www.schott.com/de-de/news-and-media/pressemitteilungen/2024/schott-produziert-optisches-glas-mit-100-prozent-wasserstoff.
[8] Incer-Valverde J, Korayem A, Tsatsaronis G, Morosuk T. "Colors" of hydrogen: Definitions and carbon intensity. Energy Convers Manage 2023;291:117294. http://dx.doi.org/10.1016/j.enconman.2023.117294.
[9] European Parliament. Directive (EU) 2023/2413 of the European parliament and of the council amending directive (EU) 2018/2001 regarding renewable energy promotion. 2023.
[10] Brandt J, Iversen T, Eckert C, Peterssen F, Bensmann B, Bensmann A, Beer M, Weyer H, Hanke-Rauschenbach R. Cost and competitiveness of green hydrogen and the effects of the European Union regulatory framework. Nat Energy 2024;9(6):703–13. http://dx.doi.org/10.1038/s41560-024-01511-z.
[11] others B. Deutsche Energie-Agentur GmbH, Preisleitfaden Green PPA: Ein Leitfaden Fuer Stromerzeuger, -Abnehmer Und Projektfinanzierer. Technical Report, DENA; 2022.
[12] Mittler C, Bucksteeg M, Staudt P. Review and morphological analysis of renewable power purchasing agreement types. Renew Sustain Energy Rev 2025;211:115293. http://dx.doi.org/10.1016/j.rser.2024.115293.
[13] Pedretti L, Kanellakopoulou M. European PPA market outlook 2024. 2023.
[14] Leo E, Dalle Ave G, Harjunkoski I, Engell S. Stochastic short-term integrated electricity procurement and production scheduling for a large consumer. Comput Chem Eng 2021;145:107191. http://dx.doi.org/10.1016/j.compchemeng.2020.107191.
[15] Gorbach OG, Thomsen J. Comparing the Energy System of a Facility with Uncertainty about Future Internal Carbon Prices and Energy Carrier Costs Using Deterministic Optimisation and Two-Stage Stochastic Programming. Energies 2022;15(10):3836. http://dx.doi.org/10.3390/en15103836.
[16] Aachen IR. Battery Charts. 2025, https://battery-charts.rwth-aachen.de/.
[17] Gabrielli P, Aboutalebi R, Sansavini G. Mitigating financial risk of corporate power purchase agreements via portfolio optimization. Energy Econ 2022;109:105980. http://dx.doi.org/10.1016/j.eneco.2022.105980.
[18] Riepin I, Brown T. System-Level Impacts of 24/7 Carbon-Free Electricity Procurement in Europe. Zenodo; 2022, http://dx.doi.org/10.5281/zenodo.7180098.
[19] Casas Ferrús MN, Ruhnau O, Madlener R. Portfolio Effects in Green Hydrogen Production Under Temporal Matching Requirements. 2024, http://dx.doi.org/10.2139/ssrn.4747405,
[20] Gabrielli P, Hilsheimer P, Sansavini G. Storage power purchase agreements to enable the deployment of energy storage in Europe. IScience 2022;25(8):104701. http://dx.doi.org/10.1016/j.isci.2022.104701.

[21] Matute G, Matute G, Yusta J, Yusta JM, Naval N, Naval N. Techno-economic model and feasibility assessment of green hydrogen projects based on electrolysis supplied by photovoltaic PPAs. Int J Hydrog Energy 2022. http://dx.doi.org/10.1016/j.ijhydene.2022.11.035.

[22] Wang Y, He X, Liu Q, Razmjooy S. Economic and technical analysis of an HRES (Hybrid Renewable Energy System) comprising wind, PV, and fuel cells using an improved subtraction-average-based optimizer. Heliyon 2024;10(12):e32712. http://dx.doi.org/10.1016/j.heliyon.2024.e32712.

[23] Wolf N, Neuber R, Mädlow A, Höck M. Techno-economic analysis of green hydrogen supply for a hydrogen refueling station in Germany. Int J Hydrog Energy 2025. http://dx.doi.org/10.1016/j.ijhydene.2025.01.424.

[24] Li Y, Huang G, Baetz B. Environmental management under uncertainty - An internal-parameter two-stage chance-constrained mixed integer linear programming method. Environ Eng Sci 2006;23(5):761–79. http://dx.doi.org/10.1089/ees.2006.23.761.

[25] Bazaraa MS, Jarvis JJ, Sherali HD. Linear Programming and Network Flows. John Wiley & Sons; 2011.

[26] Wientzek D. List of services and prices of EEX AG. 2024.

[27] van Rossum G. Python tutorial. Technical Report CS-R9526, (CS-R9526). Amsterdam: Centrum voor Wiskunde en Informatica (CWI); 1995.

[28] ISE F. Energy-Charts. 2024, https://www.energy-charts.info.

[29] DWD. Climate Data Center. 2024, https://www.dwd.de/EN/climate_environment/cdc/cdc_node_en.html,

[30] Stein JS, Holmgren WF, Forbess J, Hansen CW. PVLIB: Open source photovoltaic performance modeling functions for Matlab and Python. In: 2016 IEEE 43rd photovoltaic specialists conference (PVSC). 2016, p. 3425–30. http://dx.doi.org/10.1109/PVSC.2016.7750303.

[31] Haas S, Krien U, Schachler B, Bot S, Zeli V, Maurer F, Shivam K, Witte F, Rasti SJ, Seth, Bosch S. Wind-python/windpowerlib: Update release. 2024, http://dx.doi.org/10.5281/zenodo.10685057.

[32] Jost D, Reinert C, von der Aßen NV, Kanzurova S. Decarbonization potential of the glass melting process via energy efficiency measures and fuel switching. Technical Report RWTH-2023-02320, Lehrstuhl für Technische Thermodynamik und Institut für Thermodynamik; 2024, http://dx.doi.org/10.18154/RWTH-2023-02320.

[33] Jost D, Kanzurova S, Nilges B, Reinert C, von der Assen N. Life Cycle Assessment of Measures towards a Carbon-Neutral Glass Production. 2024, http://dx.doi.org/10.2139/ssrn.5144983, arXiv:5144983.

[34] Kalchschmid V, Erhart V, Angerer K, Roth S, Hohmann A. Decentral Production of Green Hydrogen for Energy Systems: An Economically and Environmentally Viable Solution for Surplus Self-Generated Energy in Manufacturing Companies? Sustainability 2023;15(4):2994. http://dx.doi.org/10.3390/su15042994.

[35] UMCO. Hinweise zu Mengenschwellen beim Umgang mit Wasserstoff. 2022, https://www.umco.de/blog/umweltschutz/Hinweise-Mengenschwellen-Umgang-Wasserstoff.html.

[36] Neitz-Regett A. CO_2-monitor white paper. 2024.

[37] Thomas H, Marian A, Chervyakov A, Stückrad S, Rubbia C. Efficiency of superconducting transmission lines: An analysis with respect to the load factor and capacity rating. Electr Power Syst Res 2016;141:381–91. http://dx.doi.org/10.1016/j.epsr.2016.07.007.

[38] Koltermann L, Cortés MC, Nsir N, van Ouwerkerk J, Sauer DU. Performance Testing of a Megawatt-Scale Battery Storage for Energy Trading. In: International renewable energy storage and systems conference (IRES 2023). Atlantis Press; 2024, p. 4–11. http://dx.doi.org/10.2991/978-94-6463-455-6_2.

[39] Sauer DU, Elsner P, Arzberger I, Bolt H, Doetsch C, Salinger R, Tübke J, Weidner E, Weinhold M, Burfeind J, Czyperek M, Eck M, Eichel R-A, Krassowski J, Linder M, Lunz B, Wörner A, Zunft S, Erlach B, Merzkirch M. Energiespeicher - Technologiesteckbrief zur Analyse „Flexibilitätskonzepte für die Stromversorgung 2050“. 2015, http://dx.doi.org/10.13140/RG.2.1.1478.4409.

[40] Figgener J, Hecht C, Haberschusz D, Bors J, Spreuer KG, Kairies K-P, Stenzel P, Sauer DU. The development of battery storage systems in Germany: A market review (status 2023). 2023, http://dx.doi.org/10.48550/arXiv.2203.06762, arXiv:2203.06762.

[41] Figgener J, Haberschusz D, Kairies K-P, Wessels O, Tepe B, Ebbert M, Herzog R, Sauer DU. Wissenschaftliches Mess- und Evaluierungsprogramm Solarstromspeicher 2.0. Jahresbericht 2017. 2017, http://dx.doi.org/10.13140/RG.2.2.16917.42727.

[42] Schmidt O, Gambhir A, Staffell I, Hawkes A, Nelson J, Few S. Future cost and performance of water electrolysis: An expert elicitation study. Int J Hydrog Energy 2017;42(52):30470–92. http://dx.doi.org/10.1016/j.ijhydene.2017.10.045.

[43] van der Roest E, Bol R, Fens T, van Wijk A. Utilisation of waste heat from PEM electrolysers–Unlocking local optimisation. Int J Hydrog Energy 2023;48(72):27872–91. http://dx.doi.org/10.1016/j.ijhydene.2023.03.374.

[44] Agency IE. The future of hydrogen - analysis. 2019, https://www.iea.org/reports/the-future-of-hydrogen,

[45] Abdin Z, Tang C, Liu Y, Catchpole K. Large-scale stationary hydrogen storage via liquid organic hydrogen carriers. IScience 2021;24(9):102966. http://dx.doi.org/10.1016/j.isci.2021.102966.

[46] Moradi R, Groth KM. Hydrogen storage and delivery: Review of the state of the art technologies and risk and reliability analysis. Int J Hydrog Energy 2019;44(23):12254–69. http://dx.doi.org/10.1016/j.ijhydene.2019.03.041.

[47] Ghosh PC, Emonts B, Janßen H, Mergel J, Stolten D. Ten years of operational experience with a hydrogen-based renewable energy supply system. Sol Energy 2003;75(6):469–78. http://dx.doi.org/10.1016/j.solener.2003.09.006.

[48] Germany S-GR. Data/Information from the site operator. 2024.

[49] Tschöpel H, Snellen A, Schöniger S. KPMG Cost of Capital Study. 2024, https://kpmg.com/de/en/home/insights/overview/cost-of-capital.study.html,

[50] Bank EC. ECB Data Portal: Harmonised Index of Consumer Prices (HICP). 2023, https://data.ecb.europa.eu/data/data-categories/prices-macroeconomic-and-sectoral-statistics/measuring-inflation-harmonised-index-consumer-prices-hicp/harmonised-index-consumer-prices-hicp/goods.

[51] ENTSO-E. Transparency platform. 2025, https://newtransparency.entsoe.eu/,